Chapter 9
Reduction in Harmonics for PV-Based Reduced Device Count Multilevel Inverter Wıth Genetic Algorithm

Yatindra Gopal, Kaibalya Prasad Panda, Y. N. Vijay Kumar, and G. V. Pradeep

Abstract Production of renewable energy sources (RES) has been exponential in the present years and is essentially driven by factors like the escalation of greenhouse emissions with depleting in fossil fuel reservoirs. Photovoltaic (PV) energy, a prominent RES, produces electricity directly from sunlight. Nowadays, multilevel inverter (MLI) is broadly worn in incorporation with RES and drives application. Among various RESs, PV energy is the most generous and reliable. In this manuscript reduced device count multilevel inverter (RDC MLI) incorporate with PV system with maximum power point tracking technique (MPPT) and compared with cascaded multilevel inverter (CHB MLI). Based on genetic algorithm (GA), selected harmonic elimination (SHE) technique is considered for generate the proper firing angles of PV support MLIs. The obtained firing angles are suitable to reduce the total harmonic distortion (THD) of MLIs. The PV with RDC MLI is produced less THD as compared to PV CHB MLI. Analysis of results is based on MATLAB/Simulink software platform.

Keywords Reduced device count multilevel inverter (RDC MLI) · Selected harmonic elimination pulse width modulation technique (SHEPWM) · Total harmonic distortion (THD) · Genetic algorithm (GA)

Y. Gopal (✉) · Y. N. Vijay Kumar · G. V. Pradeep
Deptament of Electrical and Electronics Engineering, SVCT, Chittoor, AP, India
e-mail: ygopal.phd@rtu.ac.in

K. P. Panda
Department of Electrical Engineering, National Institute of Technology, Meghalaya, Shillong, Meghalaya, India
e-mail: kaibalyapanda@nitm.ac.in

G. Panda et al. (eds.), *Sustainable Energy and Technological Advancements*,
Advances in Sustainability Science and Technology,
https://doi.org/10.1007/978-981-16-9033-4_9

1 Introduction

Generation of energy from RES has been exponential in current years and is essentially driven by factors like the escalation of greenhouse emissions with depleting in fossil fuel reservoirs [1–3]. Photovoltaic (PV) energy, a prominent RE source, produces electricity directly from sunlight. Its operation is noiseless and harmless to the environment. The PV system is interfaced with various essential power electronic components to achieve necessary efficiency in energy conversion to harness renewable energy.

Controlling the output voltage of PV cells varies when regulating the irradiation and environmental [4–7]. Hence, the necessity of MPPT technique and boost converter is considered to generate desired output voltage by PV cells. A variety of control techniques has been worn to discover the maximum power point (MPP). Perturbation and observation (P&O) technique is very easy and simplicity with simple implementation. P&O works based on iterative method, and it swings near the point $dP/dV = 0$, i.e., MPP. Incremental conductance (IC) technique gives the best dynamic performance and accuracy when fast change in atmospheric environment. In this paperwork, IC MPPT is worn with the adaptive distinction in size of steps. IC method used to solve the difficulty of conventional process when the irradiance changes. IC method evaluates with some further variable step size methods; the worn method is not complex instruction coefficient and estimates to progress the computing speed.

Voltage production by PV is not efficient for network rating and hence considers the DC-DC boost converters to boost the PV panels output. The boost output voltage in form of DC, but requirements in commercial purpose in form of AC seeing as most of the loads are AC loads.

Hence, MLI topologies are used to produce AC voltages to improve the voltage performance with less THD [8–11].

CHB MLI, diode-clamped inverter (DCI), and capacitor-clamped inverter (CCI) are very common topologies and fine expression in the literature [12–15]. CHB MLI has various advantages compared to the conventional MLIs but requirements of devices are more. Hence, RDC MLI configuration topology with GA is used in this paper to minimize the THD.

The number of devices in MLI increases, and then cost, circuit configuration, and reliability also increase. Hence, the configuration of MLIs with less number of devices is the key element [16–29]. To generate the same output voltage levels such as 7-level (7L) CHB MLI, a novel configuration is designed with 7L-RDC MLI devoid of raising the number of bridges.

In this manuscript, SHE technique is taken to solve the nonlinear equations and produced the best results of MLIs. In addition, this manuscript reports the on PV 7-level (7L) RDC MLI topology; this process requires less switches and devices. The voltage produced by 7L-RDC MLI similar voltage output generates via 7L-CHB MLI.

In this work, estimating the values of switching angles is through solving of transcendental nonlinear equations with using GA. Newton–Raphson (NR) and resultant theory (RT) method suffer from some disadvantages to calculate the optimal value of switches [15]. NA and RT methods are not suitable when it applied to higher level MLIs. Hence, in this work bio-inspired optimization method-based GA SHE is used to the development of the system robustness.

GA is useful to solve the constrained and unconstrained troubles through the suitable assortment of unique population and gradually regularly adjust the individual population. By GA, find out the optimal values of angles of PV-based 7-L CHB MLI and 7L-RDC MLI, this work is performed the minimum value of THD.

2 Modeling of PV Cell

The simple way to represent a photovoltaic cell is with one diode model [2]. It consists of parallel with the current to a diode and required parameters such as diode identity factor (a), (V_{oc}) open-circuit voltage, and (I_{sc}) short-circuit current.

The realized characteristics of PV cell by the fundamental equation of a one cell as the source of current are placed in parallel by diode. The current output Eq. 1 is as follows:

$$I = I_{PV} - I_o\left[e\frac{q(V + IR_s)}{akT} - 1\right] - \left[\frac{V + IR_s}{R_\rho}\right] \tag{1}$$

I_{PV} is the function of irradiance (G) and the mathematical calculation of PV current is given as in Eq. 2

$$I_{PV} = \left[I_{PV\_STC} + K_i \Delta T\right]\frac{G}{G_{STC}} \tag{2}$$

The saturation current (I_o) of diode is formulated in Eq. 3 as follows:

$$I_o = I_{o\_STC}\left(\frac{T}{T_{STC}}\right)^3 \exp\left[\frac{qEg}{ak}\left(\frac{1}{T_{STC}} - \frac{1}{T}\right)\right] \tag{3}$$

The flowchart representation of the PV current calculation is given in Fig. 1. The detailed outputs of PV model are shown in Fig. 2.

3 Modeling of Boost Convertors

Boost convector is known as step-up convertor which converts DC to DC power [2]. This is similarly to switched mode power supply (SMPS) among a diode, a transistor

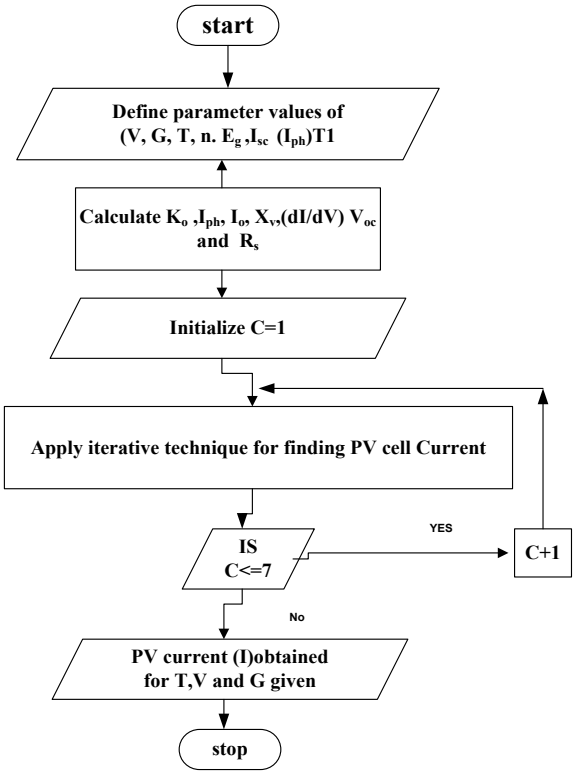

Fig. 1 Flowchart of PV cell current calculation

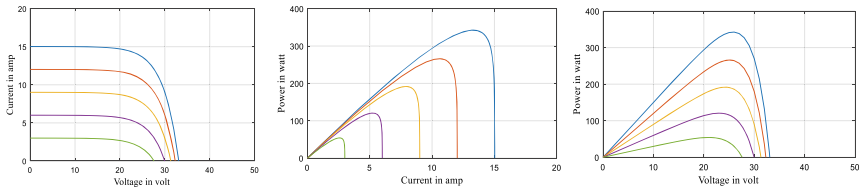

Fig. 2 Output of the PV model

with storage element of energy such as capacitor and inductor. The basic principle of boost convertor is that it can work in two modes. The first one is when the switch is working mode, then energy stores in inductor and energy releases by capacitor. In case when switch is not working, then energy stores in capacitor and released by the inductor. The voltage across the inductor is mathematically given as represented in Eq. 4.

$$v_{\mathrm{L}} = V_{\mathrm{s}} = L\frac{\mathrm{d}i_{\mathrm{L}}}{\mathrm{d}t}$$
$$\frac{V_{\mathrm{s}}}{L} = \frac{\mathrm{d}i_{\mathrm{L}}}{\mathrm{d}t} \tag{4}$$

4 Incremental Conductance Method

IC is the method with the high performance, increased tracking speed better efficiency, and ease in implementation [2].

The basic idea in IC algorithm is that slop of the PV curve becomes zero on MPP. The slope of PV derivative power with respect to the voltage of PV has successive relation with MPP [1, 2].

$\frac{\Delta P}{\Delta V} = 0$ at MPP, $\frac{\Delta P}{\Delta V} > 0$ left side for MPP,

$$\frac{\Delta P}{\Delta V} < 0 \quad \text{Right side for MPP} \tag{5}$$

$$\text{At the MPP}: \frac{\mathrm{d}I}{\mathrm{d}V} = -\frac{I}{V} \tag{6}$$

When working point left side for MPP:

$$\frac{\mathrm{d}I}{\mathrm{d}V} > -\frac{I}{V} \tag{7}$$

When working point right side for MPP:

$$\frac{\mathrm{d}I}{\mathrm{d}V} < -\frac{I}{V} \tag{8}$$

where $\mathrm{d}I/\mathrm{d}V$ is IC and $\frac{I}{V}$ is instantaneous conductance; MPP is found by evaluate instantaneous conductance to the IC. The pictorial form of the IC is shown in Fig. 3, and comparisons of different MPPT techniques are shown in Table 1.

MPPT methods are key enablers of an extra energy sustainable culture, due to their utilization ease, low cost, and malleable operation. The analysis is done on variable irradiance and temperature conditions. It is observed that IC has better performance than P&O techniques.

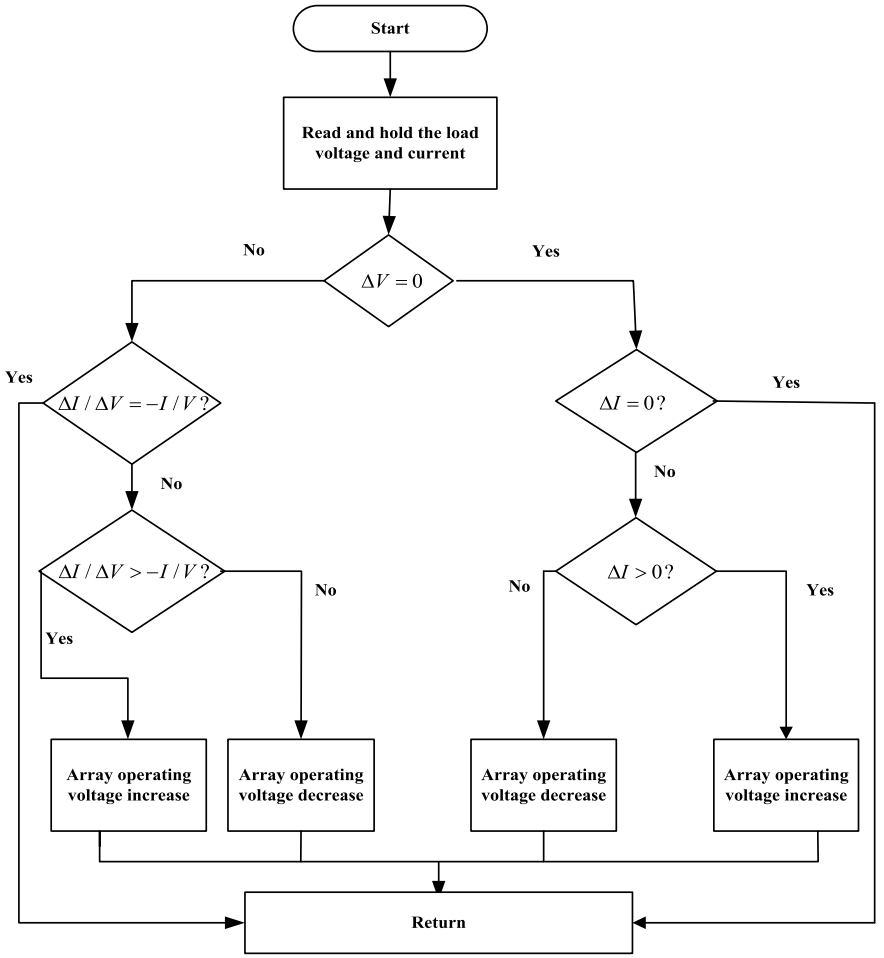

Fig. 3 Flowchart of IC method

5 PV 7L-CHB MLI Topology

CHB MLI modular topology gives the preferred output voltage, power with higher stability. Modular topology feature enables each inverter to be a module with a comparable circuit topology, power arrangement, and modulation [9, 11]. Each inverter level gives three different output voltages, i.e., $+ V_{dc}$, 0 or $- V_{dc}$ [12]. Three-level structure investigated by [12], and total voltage positive half cycle is $+ 3V_{dc,}$ and in negative, half cycle is $-3V_{dc}$. The number of output phase voltage steps is calculated via $n = (2\ k + 1)$, and here k defines number of DC supply. The PV 7L-CHB MLI configuration scheme is shown in Fig. 4. This configuration produced 7L voltage steps with the use of 12 IGBTs electronics device and 3 DC supply. MLI switching function with 12 switches and 3 DC supply is shown in Table 2.

Table 1 Different of MPPT techniques

S. No.	Methods comparative area	Short circuit current	Short circuit voltage	P&O	IC
1	Tracking speed	Low	Low	Low	High
2	Convergence speed	Average	Average	Average	High
3	Hardware implementation	Easy	Easy	Easy	Easy
4	Level of complexity	High	High	Low	Low
5	Effect on hardware	May damage	May damage	Secure	Secure
6	Power loss	More	More	Medium	Less

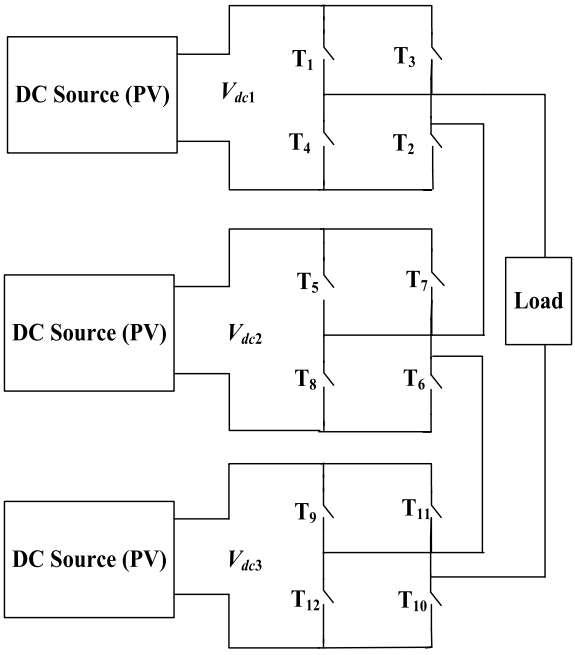

Fig. 4 Configuration of 1-ϕ 7L-CHB MLI with PV scheme

6 PV 7L-RDC MLI Topology

In MLIs, the number of switches represents the price, volume of circuit, reliability, and complexity. So the number of necessary switches to generate the essential voltage level is necessary to designing a MLI. To achieve the same output in 7L-CHB MLI, a novel structure is configured and less count of number of switches exclusive of rising the number of H-bridges. Figure 5a shows the proposed MLI structure, and Fig. 5b

Table 2 Switching function of 7L-CHB MLI

Switching condition	T_1	T_2	T_3	T_4	T_5	T_6	T_7	T_8	T_9	T_{10}	T_{11}	T_{12}
$+3V_{dc}$	1	1	0	0	1	1	0	0	1	1	0	0
$+2V_{dc}$	1	1	0	0	1	1	0	0	0	0	0	0
$+V_{dc}$	1	1	0	0	0	0	0	0	0	0	0	0
0	0	0	0	0	0	0	0	0	0	0	0	0
$-V_{dc}$	0	0	1	1	0	0	0	0	0	0	0	0
$-2V_{dc}$	0	0	1	1	0	0	1	1	0	0	0	0
$-3V_{dc}$	0	0	1	1	0	0	1	1	0	0	1	1

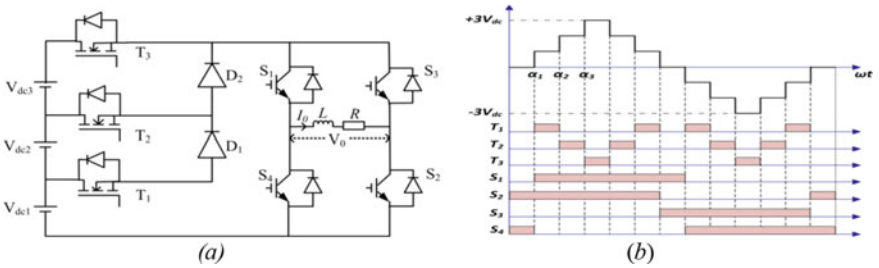

Fig. 5 Seven-level RSMLI and its output voltage **a** Structure of 7L-RDC MLI, **b** Output voltage waveform with corresponding switching condition

shows the novel MLI voltage waveform with consequent switching condition. The switches operation (or polarity generation switches) is working at low switching frequency while the steps formation switches T_1–T_3 working at high switching frequency. Consequently, a price efficient solution is to choose lower switching power equipments of the H-bridge and high switching power equipments for the steps formation.

In comparison with a 7L-CHB MLI, the required number of switches in 7L-RS MLI is very less. In 7L-CHB MLI, 12 switches are used, whereas only 7 switches with 2 discrete diodes are used in design of 7L-RDC MLI. The 7L-RDC MLI working principle is summarized in the following modes.

Mode (a): When T_1 is ON, the current flows through two diodes and H-bridge switches S_1 and S_2. Output voltage at load is $+V_{dc}$. Similarly, S_3 and S_4 are switched ON, and voltage output is $-V_{dc}$.

Mode (b): In this mode, switch T_2 is make ON and then path of current through diode D_2, switches S_1 and S_2. Output voltage at load is $+2V_{dc}$. Similarly, S_3 and S_4 are switched ON, and voltage output is $-2V_{dc}$.

Mode (c): T_3 is ON, and this mode of operation starts. Path of current is switches S_1 and S_2. Output voltage at load is $+3V_{dc}$. Diodes D_1 and D_2 are not performed operation. Similarly, S_3 and S_4 are switched ON, and voltage output is $-3V_{dc}$.

Table 3 Switching scheme of 7L-RSC-MLI

Switching state	T_1	T_2	T_3	S_1	S_2	S_3	S_4	D_1	D_2
$+3V_{dc}$	0	0	1	1	1	0	0	Off	Off
$+2V_{dc}$	0	1	0	1	1	0	0	Off	On
$+V_{dc}$	1	0	0	1	1	0	0	On	On
0	0	0	0	1	0	1	0	Off	Off
0	0	0	0	0	1	0	1	Off	Off
$-V_{dc}$	1	0	0	0	0	1	1	On	On
$-2V_{dc}$	0	1	0	0	0	1	1	Off	On
$-3V_{dc}$	0	0	1	0	0	1	1	Off	Off

Mode (d): Any set of S_1 and S_3 or S_2 and S_4 are ON in this mode. Switches T_1, T_2, and T_3 are in OFF condition. Obtained load across voltage is zero.

The RSC-MLI switching scheme is represented in Table 3. The voltage is obtained from a RSC-MLI with corresponding switching states is depicted in Fig. 5a, b.

7 Calculation of THD Using Optimization Algorithm

As described earlier, the SHE technique significantly makes to produce the output voltage of MLIs. MLIs voltage output waveform is positive half is equal to the negative half, i.e., exhibits quarter symmetrical output. The formation of output voltage waveform is shown in Fig. 7b, and it can be defined in Fourier form as,

$$V(\mathrm{t}) = \sum_{n=1}^{\infty} V_n \sin(n\alpha_n) + B_n \cos(n\alpha_n) \tag{9}$$

The even harmonics usual canceled because it is quarter-wave symmetry, i.e., $B_n = 0$ for all n. So the novel equation of output voltage becomes

$$V(\mathrm{t}) = \sum_{n=1}^{\infty} V_n \sin(n\alpha_n) \tag{10}$$

The amplitude V_n can be defined in terms of Fourier form with α varying in the range 0 to $\pi/2$,

$$V_n = \frac{4V_{dc}}{n\pi}(\cos n\alpha_1 + \cos n\alpha_2 + \cos n\alpha_3) \tag{11}$$

Three switching angles α_1,α_2, and α_3, the fundamental component of output voltage is adjust by the modulation index (M). The dominant lower order harmonics

is necessary to eliminate from the output voltage. Accordingly, the three nonlinear equations for elucidation of the problem are used in this paperwork as:

$$\begin{aligned} V_1 &= \frac{4V_{\mathrm{dc}}}{\pi}(\cos\alpha_1 + \cos\alpha_2 + \cos\alpha_3) = m \\ V_5 &= \frac{4V_{\mathrm{dc}}}{5\pi}(\cos 5\alpha_1 + \cos 5\alpha_2 + \cos 5\alpha_3) = 0 \\ V_7 &= \frac{4V_{\mathrm{dc}}}{7\pi}(\cos 7\alpha_1 + \cos 7\alpha_2 + \cos 7\alpha_3) = 0 \end{aligned} \tag{12}$$

where$m = \frac{V_f}{(4V_{\mathrm{dc}}/\pi)}$, modulation index $= M = m/N_{\mathrm{DC}}$ and N_{DC} is the number of DC sources, V_f is the required value of fundamental voltage.

Fifth- and seventh-order harmonics are targeted to eliminate by solving the above nonlinear as Eq. 13. The solution of these equations leads to discontinuity for the certain modulation index. Conventional technique such as NR method is able to solve these problems involves much calculation time and difficult mathematical arrangement. In order to reduce this, GA is used here to solve the objective function to find the best value of switching angles. The optimal fitness function (FF) is taken to remove the 5th and 7th component harmonics at optimal values of switching angles. Fundamental component equation goes as under:

$$\mathrm{FF} = \frac{1}{h} * \left[\left| M - \frac{|V_1|}{N_{\mathrm{DC}} V_{\mathrm{DC}}} \right| + \left(\frac{|V_5| + |V_7|}{N_{\mathrm{DC}} V_{\mathrm{DC}}} \right) \right] \tag{13}$$

Subject to condition that,

$$0 < \alpha_1 < \alpha_2 < \alpha_3 < \frac{\pi}{2} \tag{14}$$

To obtain least THD with possible modulation index, the total set is multiplied with a factor $\frac{1}{h}$. The target of this paper, 5th and 7th harmonics are set under the error limit 1% (i.e., $h = 0.01$). To analyze the superiority of voltage THD, it can express and calculated as under:

$$\mathrm{THD}\,(\%) = \left[\frac{1}{V_1^2} \sum_{k=2}^{\infty} (V_k)^2 \right]^{\frac{1}{2}} \times 100 \tag{15}$$

where V_k is the voltage of exacting harmonics.

8 Genetic Algorithm (GA)

In this section, GA results obtained for the switching angles of 7L-CHB MLI and 7L-RDC MLI are described. GA [15] is the method of random search process used to find optimal solutions of optimization problems. This is a search technique inspired by biological evolution, such as selection, crossover, and mutation. Usually, evolution starts from a random initial population and repeatedly modifies the solution in each of generation. Multiple switching angles are selected over the successive generation from current population and are used in the next iteration of the algorithm. It is repeated till an optimal solution is reached with defined accuracy.

With continuous number of generations and a large population in each production, the algorithm finally finds for a set of solutions of the problem. It computes the different values of three switching angles to obtain the minimum *FF* keeping the harmonics within the limit. Flowchart collection of the GA shown in Fig. 6 represents the different steps for calculation of FF values.

The GA toolbox results obtained from GA are summarized in Table 4. To use GA toolbox, The following information are entered.

Fitness function: The FF as given entered in the form @FF, where FF.m is a program file that computes the FF.

No of variables: The length of input vector to the FF is entered. Three switching angles are considered as variables.

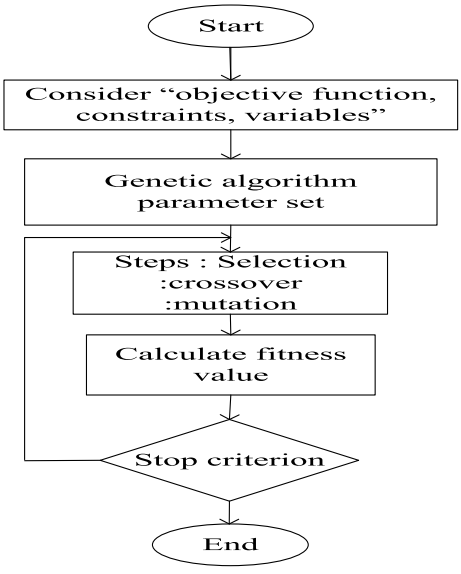

Fig. 6 Flowchart arrangement of the GA

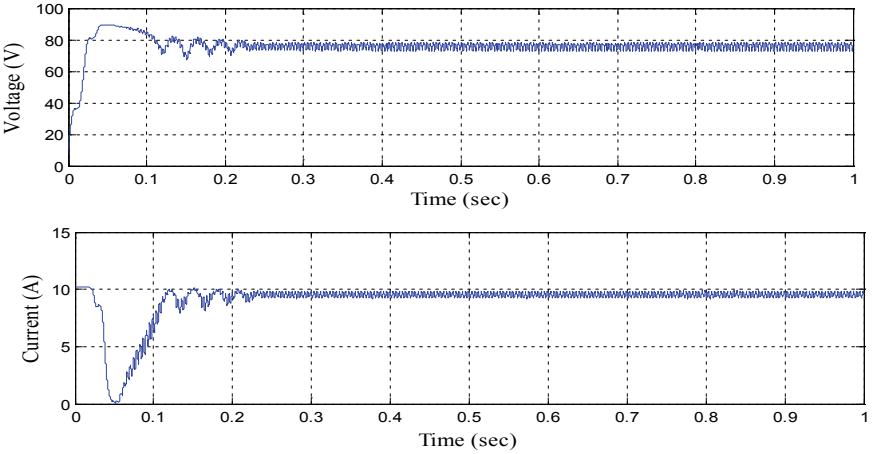

Fig. 7 Output voltage (V) and current (A) of PV system

Table 4 Results obtained from GA FOR 7L-MLIS

Results obtained from GA	Generation count	Obtained switching angles (in degree)			Mean fitness	Best fitness
	100	α_1	α_2	α_3	0.133	0.088
		12.56	49.69	56.89		

Constraint function for the problems is specified in **constraints pane** of toolbox. Boundary variable for the variable is also specified. Population size, initial population, and command are set in the **options pane.**

9 Results and Analysis

The configuration of PV, boost converter (DC-DC), and IC MPPT integrated with MLI is designed at MATLAB platform. The generated voltage and current output by PV without boost voltage are shown in Fig. 7.

The voltage should be increased for each PV panel as shown in Fig. 8. The PV output voltage of 7L-RDC MLI interfaces with boost converter is shown in Fig. 8.

The simulated output voltage is observed from 7L-CHB MLI and 7L-RDC MLI as shown in Fig. 9a, b.

FFT analysis of THD present in 7L- CHB MLI output voltage is 15.50% and 7L-RDC MLI 10.36% at the fundamental frequency of 50 Hz which is as shown in Fig. 10. The comparisons of MLIs performance and different MPPT control schemes are shown in Table 5.

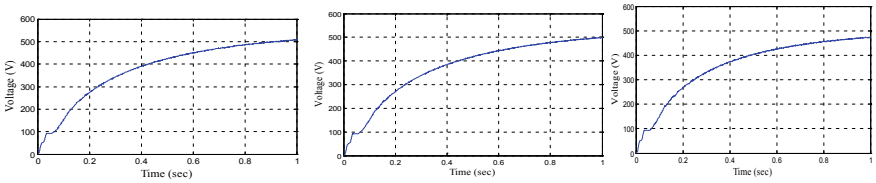

Fig. 8 Output of 7L-CHB MLI between boosted voltage (V) and time (s) of **a** PV panel[1], **b** PV panel[2], and **c** PV panel[3]

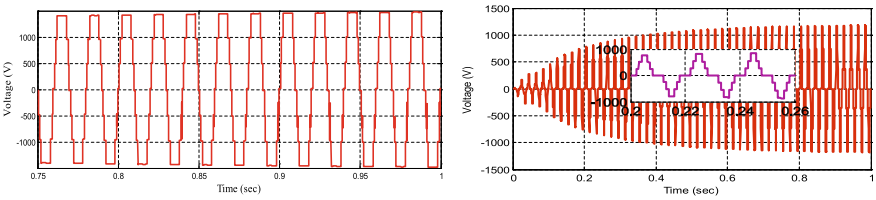

Fig. 9 **a** Overall output voltage of 7L-CHB MLI, **b** 7-L RDC MLI

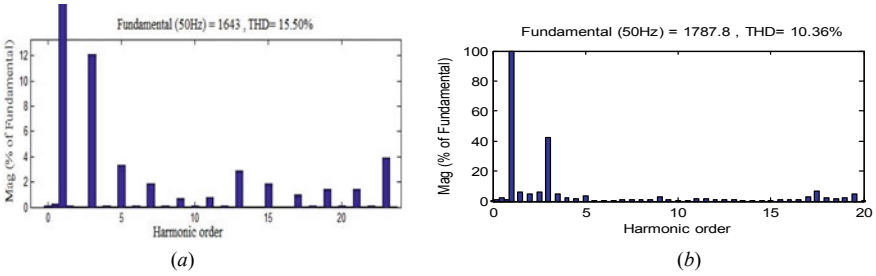

Fig. 10 FFT analysis of THD present in the voltage output for **a** 7L-CHB MLI, **b** 7-L RDC MLI

Using a new 7L-RDC MLI topology reduced switch count was presented and also compared with the conventional 7L-CHB MLI. The total number of switches is almost halved as compared to the CHB MLI topology. So, switching loss is expected to be reduced significantly and cost is also less.

10 Conclusion

This paperwork describes 1-ϕ PV 7L-RDC MLI and 7L-CHB MLI with DC-DC converters, IC control technique and compared it. The feature of PV-based 7L-RDC MLI plays the important role for produce the sufficient power to fulfill the load

Table 5 A comparison of MLIS performance and MPPT

S. No.	Property	Performance
1	Convergence speed (P&O)	More
2	Convergence speed (IC)	Medium
3	Oscillation close to MPP (P&O)	More
4	Oscillation close to MPP (IC)	Medium
5	Implementation complexity	Easy
6	Power loss	Less
7	PV 7L-CHB MLI circuit voltage THD	15.50%
8	PV 7L RSC-MLI circuit voltage THD	10.36%
9	Power semiconductor switches 7L-CHB MLI circuit	12
10	Power semiconductor switches 7L-RDC MLI circuit	7
11	Unbalancing voltage 7L-CHB MLI circuit	Very small
12	Unbalancing voltage 7L-RDC MLI circuit	Very less

demand with fewer number of semiconductor switches. The THD performance of output voltage is improved with less number of components reducing the volume, size, and price of MLIs. The MLIs have less the %THD without any filter circuit requirement. GA optimization technique is used to faster response with less time-consuming. SHE equation of MLIs is solved by GA toolbox, and simulation is done at MATLAB platform. From the calculated results by simulation, it clarifies GA-based SHE technique can be useful to MLI. When the level of MLI is increased, the output voltage waveform just goes to smooth sinusoidal appearance and also decreases the THD.

References

1. Roy T, Kumar PS (2021) A step-up multilevel inverter topology using novel switched capacitor converters with reduced components. Trans Circuits Syst II: Express Briefs 68:236–247
2. Tamrakar V, Gupta S, Sawle Y (2015) Single-diode and two-diode Pv cell modeling using matlab for studying characteristics of solar cell under varying conditions. Electr Comput Eng Int J 4:67–77
3. Upadhyaye H, Gopal Y, Birla D (2019) THD Analysis for PV based cascaded multilevel inverters with MPPT technique. In: Proceedings of international conference on sustainable computing in science, technology and management (SUSCOM), Amity University Rajasthan, Jaipur - India, February 26-28, 2019. Available at SSRN: https://ssrn.com/abstract=3358061 or https://doi.org/10.2139/ssrn.3358061
4. Gopal Y, Kumar K, Birla D, Lalwani M (2017) Banes and boons of perturb & observe, incremental conductance and modified Regula Falsi methods for sustainable PV energy generation. J Power Technol 97:35–43
5. Villalva MG, Gazoli JR, Filho ER (2009) Comprehensive approach to modeling and simulation of photovoltaic arrays. IEEE Trans Power Electron 24:1198–1208

6. Jiang Y, Qahouq JAAA, Orabi M (2011) Matlab/Pspice hybrid simulation modeling of solar PV cell/module. In: 2011 twenty-sixth annual IEEE applied power electronics conference and exposition (APEC), pp 1244–1250
7. Gopal Y, Birla D, Lalwani M (2020) Reduced switches multilevel inverter integration with boost converters in photovoltaic system. SN Appl Sci 2:1–15
8. Salameh Z, Taylor D (1990) Step-up maximum power point tracker for photovoltaic arrays. Sol Energy 44:57–61
9. Shubhada Doifode D, Shend R (2015) Multilevel ınverter modeling—a brief overview. Int J Eng Manage Res 5:401–404
10. Nabae A, Takahashi I, Akagi H (1981) A new neutral-point-clamped PWM ınverter. IEEE Trans Indus Appl IA-17:518–523
11. Swami RK, Samuel P, Gupta R (2016) Power control in grid-connected wind energy system using diode-clamped multilevel inverter. IETE J Res 62:515–524
12. Panda KP, Sahu BP, Samal D, Gopal Y (2013) Switching angle estimation using GA toolbox for simulation of cascaded multilevel inverter. Int J Comput Appl 73
13. Gopal Y, Birla D, Lalwani M (2018) Selected harmonic elimination for cascaded multilevel inverter based on photovoltaic with fuzzy logic control maximum power point tracking technique. Technologies 6:2–17
14. Gopal Y, Panda KP, Birla D, Lalwani M (2016) Swarm optimization-based modified selective harmonic elimination PWM technique application in symmetrical H-bridge type multilevel inverters. Eng Technol Appl Sci Res 9:3836–3845
15. Bektas B, Karaca H (2016) GA based selective Harmonic elimination for five-level inverter using cascaded H-bridge modules. Int J Intel Syst Appl Eng 4:29–32
16. Gopal Y, Lalwani M, Birla D (2017) Genetic algorithm based cascaded H-bridge multilevel inverters for PV system with MPPT technique. In: 2017 ınternational conference on Information, communication, ınstrumentation and control (ICICIC), pp 1–6
17. Taghizadeh TH, Hagh MT (2010) Harmonic elimination of cascade multilevel inverters with non-equal DC sources using particle swarm optimization. IEEE Trans Indus Electron 57:3678–3684
18. Farokhnia PN, Fathi SH, Yousefpoor N, Bakhshizadeh MK (2012) Minimization of total harmonic distortion in a cascaded multilevel inverter by regulating voltages of DC sources. IET Power Electron 5:106–114
19. Bana PB, Panda KP, Naayagi RT, Siano P, Panda G (2019) Recently developed reduced switch multilevel inverter for renewable energy integration and drives application: topologies, comprehensive analysis and comparative evaluation. IEEE Access 7:54888–54909
20. Panda KP, Bana PR, Panda G (2020) A self-balanced switched-capacitor boost seven-level ınverter for photovoltaic systems. In: 2020 IEEE ınternational conference on computing, power and communication technologies (GUCON), pp 338–343
21. Panda KP, Lee SS, Panda G (2019) Reduced switch cascaded multilevel inverter with new selective harmonic elimination control for standalone renewable energy system. IEEE Trans Ind Appl 55(6):7561–7574
22. Panda KP, Bana PR, Panda G (2020) FPA optimized selective harmonic elimination in symmetric-asymmetric reduced switch cascaded multilevel inverter. IEEE Trans Ind Appl 56(3):2862–2870
23. Panda KP, Bana PR, Kiselychnyk O, Wang J, Panda G (2021) A single-source switched-capacitor-based step-up multilevel inverter with reduced components. IEEE Trans Ind Appl 57(4):3801–3811
24. Panda KP, Bana PR, Panda G (2020) Reduced switch count seven-level self-balanced switched-capacitor boost multilevel ınverter. In: 2020 IEEE ınternational conference on power electronics, drives and energy systems (PEDES), pp 1–6
25. Panda KP, Bana PR, Panda G (2020) A single source switched-capacitor based multilevel ınverter for photovoltaic application. In: 2020 IEEE ınternational conference on power electronics, smart grid and renewable energy (PESGRE2020), Kerala, India, pp 1–6

26. Bana PR, Panda KP, Panda G, Performance evaluation of a reduced components count single-phase asymmetric multilevel inverter with low standing voltage. Int Trans Electr Energy Syst e12239
27. Bana PR, Panda KP, Panda G (2020) Power quality performance evaluation of multilevel inverter with reduced switching devices and minimum standing voltage. IEEE Trans Industr Inf 16(8):5009–5022
28. Panda KP, Bana PR, Panda G (2020) A switched-capacitor self-balanced high-gain multilevel inverter employing a single DC source. IEEE Trans Circuits Syst II Express Briefs 67(12):3192–3196
29. Panda KP, Bana PR, Panda G (2021) A reduced device count single DC hybrid switched-capacitor self-balanced inverter. IEEE Trans Circuits Syst II Express Briefs 68(3):978–982